

Quantum key distribution component loopholes in 1500–2100 nm range perspective for Trojan-horse attacks

Boris Nasedkin,^{1, 2, *} Fedor Kiselev,^{2, 3} Ilya Filipov,² Darya Tolochko,² Azat Ismagilov,¹ Vladimir Chistiakov,^{1, 2} Andrei Gaidash,^{1, 3, 4} Anton Tsyplkin,¹ Anton Kozubov,^{1, 3, 4} and Vladimir Egorov^{2, 3}

¹*Laboratory of Quantum Processes and Measurements, ITMO University,
199034, 3b Kadetskaya Line, Saint Petersburg, Russia*

²*Laboratory for Quantum Communications, ITMO University,
199034, 3b Kadetskaya Line, Saint Petersburg, Russia*

³*SMARTS-Quanttelecom LLC, Saint Petersburg, 199178, Russia*

⁴*Department of Mathematical Methods for Quantum Technologies,*

Steklov Mathematical Institute of Russian Academy of Sciences, 119991, 8 Gubkina St, Moscow, Russia

(Dated: December 1, 2022)

Vulnerabilities of components used in quantum key distribution (QKD) systems affect its implementation security and must be taken into consideration during system development and security analysis. In this paper, we investigated transmission of fiber optical elements, which are commonly used in QKD systems for designing countermeasures against Trojan-horse attacks, in 1500–2100 nm range. As a result, we found loopholes in their transmission spectra which open possibilities for eavesdropping. We also suggested a simple passive countermeasure based on violation of total internal reflection in single-mode fiber, that leads to additional insertion losses of at least 60 dB for double-pass Trojan-horse probe pulses for wavelengths longer than 1830 nm.

I. INTRODUCTION

One of the interesting applications of quantum technology is quantum key distribution (QKD) which allows two legitimate parties to generate symmetrical bit sequences secured by laws of quantum physics. That means that an illegitimate user, or eavesdropper, usually called Eve, has no possibility of stealing the secret key while staying undetected by legitimate users (Alice and Bob), because any intermediate measurement in the quantum channel would affect the quantum bit error rate (QBER)[1–3] or the excess noise level [4] depending on the given QKD protocol. One of the main problems in practical QKD is to prove theoretical security of the given protocol.

However, even when the QKD system is designed based on a theoretically proven protocol, its technical implementation might still remain vulnerable to a vast number of attacks based on imperfections of real-life optical components [5–9], known as quantum hacking. For example, some of these attacks concentrate on heating optical elements, which leads to the change of their properties or disables them completely [10, 11], thus opening attack loopholes. Other attacks, such as the Trojan-horse attack (also known as "large pulse attack") [12–16] and detector blinding attack [17–19] (also for those attacks, where detector blinding is necessary component, e.g. [20, 21]) use high transmission spectral regions of optical elements to illegitimately interact with Alice's and Bob's setups via optical probing.

To implement Trojan-horse attack an eavesdropper directs intense optical pulses to Alice's or Bob's modules which propagate through them and interacts with the

inner optical elements used in quantum state generation and detection. A fraction of these probe pulses is reflected back to the channel, similar to optical time domain reflectometry (OTDR) [22], and may be registered by Eve, who uses suitable registration techniques, such as homodyne detection for phase-coded states. Trojan-horse attack has an upper bound of the source power used for the attack, because high intensity can destroy optical fiber before light reaches optical elements, or cause a destructive fiber fuse effect [23]. This limits the maximal probing power which is estimated approximately as 10 W, according to [10] for continuous-wave lasers, while for pulsed sources it reduced with the decrease of pulse duration. The lower bound for attack power is limited by the probability of information extraction from back reflected light (simply put, probability of at least one photon returning to Eve to make measurements). These limitations are individual for various QKD systems.

To ensure the protection of QKD systems against quantum hacking, and Trojan-horse attacks in particular, additional optical elements are introduced into the QKD modules in order to limit to detect optical pulses send by the eavesdropper. Such elements include attenuators, filters, isolators, circulators, monitor photodiodes, etc. However, these elements, in turn, have their own vulnerabilities and loopholes which were previously investigated in [24, 25] for 1000–1800 nm range. However, in practice Trojan-horse attack is feasible for wavelengths longer than 1250 nm for a single-mode fiber, as it is limited by distinguishability of the measured states and absorption of the fiber. Moreover, Trojan-horse attack may be quite effective at wavelengths longer than 1750 nm and was previously demonstrated for 1924 nm [26]. Moreover, optical probing in a wide spectral range can potentially be used in other quantum hacking techniques. However, spectral measurement of fiber optical element

* banasedkin@itmo.ru

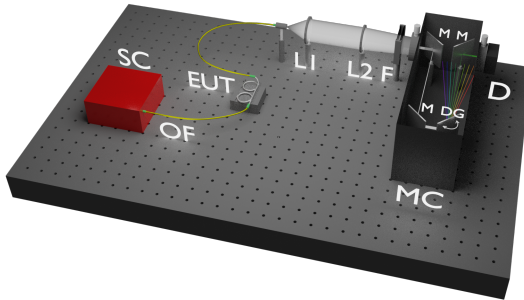


FIG. 1. Experimental setup for measuring fiber optical elements insertion loss in 1500 – 2100 nm range. SC is supercontinuum source, OF is optical fiber, EUT is element under test, L1, L2 are lenses, F are neutral spectral filters, MC is monochromator, M is mirror, DG is diffraction grating, D is photodiode detector

in such a wide range constitute an engineering problem because several precise sources and detector are needed to perform them. These measurement should be then taken into consideration during the full security analysis. Therefore measuring transmission of QKD system elements both in forward and backward directions for ranges beyond 1000 – 1800 nm constitute an important practical problem.

There are two methods of measuring transmission and reflectance of fiber optical elements. The first one is to use tunable lasers which allow to achieve higher power for a single wavelength measurement without damaging the system and consequently expand the dynamic range of the measurement [27]. The drawback of such approach is the discrete spectra of such lasers. Another way is to use broadband sources, such as thermal or supercontinuum sources [24, 28]. However, the main drawback of broadband sources is high integral intensity and low intensity at a single wavelength when compared to tunable lasers.

In this work we investigate insertion losses of several optical elements conventionally used in QKD in 1500 – 2100 nm range in search of potentially open spectral loopholes for quantum hackers using optical probing technique. It is important to note that the range from 1800 nm to 2100 nm has never been completely investigated before. We also propose a passive countermeasure which reduces the possibility of Trojan-horse attack in this spectral range and could be simply integrated into QKD systems.

II. EXPERIMENT AND RESULTS

A. Experimental setup

In our experimental setup (Fig.1) we used a pulsed supercontinuum generator (SC, Avesta EFOA) as a broadband light source with integral intensity of 150 mW [29].

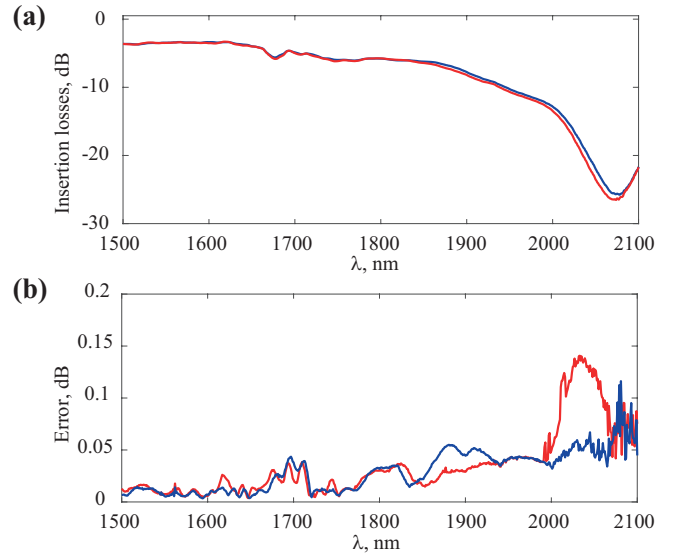


FIG. 2. Measured insertion losses and calculated error for phase modulator. (a) Insertion losses for phase modulator. Blue line is insertion losses in forward direction, red line is insertion losses in backward direction; (b) error for phase modulator. Blue line is insertion losses in forward direction, red line is insertion losses in backwards direction.

Light from this source was guided in a single-mode fiber (OF) to investigate different fiber optical elements under test (EUT). Then, transmitted light was collimated into a free space monochromator (MC, Action 2500) and measured by a calibrated photodiode (D, Hamamatsu). One of the problems of measurements in the optical range beyond the telecommunication range is lack of equipment with high dynamic range. To solve this issue, transmitted light was attenuated utilizing two conventional neutral spectral filters (NS10 and NS11) with known attenuation in the broadband spectral range. Since dynamic range of utilized photodiodes is low (~ 30 dB), we measured lower intensities by removing the filters. Then, the insertion losses were recalculated according to the formula:

$$T_{dB} = -10 \log_{10}(I_{ref} * T_f / I_{mes}), \quad (1)$$

where I_{ref} is measured intensity without element under test, I_{mes} is measured intensity with element under test, T_f is filter transmission.

In our experiment we used subcarrier wave QKD testbed described in [30]. To collect the data needed for security proof against Trojan-horse attack we measured individual insertion losses of optical elements included in the system in forward and backwards direction. To find overall insertion loss for Alice and Bob setups we summed up the losses on individual elements. Final results were averaged by 10 measurements, and errors were calculated. Note that we measured only optical elements placed before phase modulator based on assumption of maximal reflection (of eavesdropper's optical probe) was

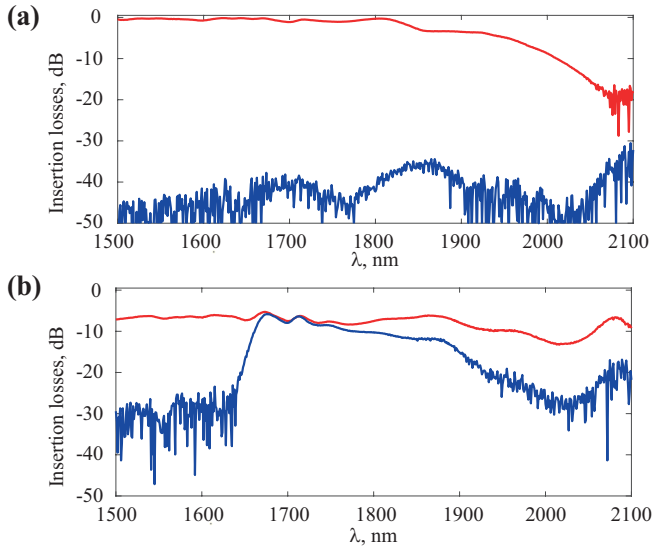


FIG. 3. Measured insertion losses of variable optical attenuators. (a) For Electro-optical VOA (red line is insertion losses without any attenuation, blue line is insertion losses maximal attenuation); (b) for electro-mechanical VOA (red line is insertion losses without any attenuation, blue line is insertion losses maximal attenuation)

at the modulator crystal facet. We assumed it to be about $\text{Ref} = -50 \text{ dB}$ for each studied wavelength [26].

B. Experimental results

1. Phase modulator

Phase modulator (PM) is present in virtually any QKD system with phase encoding, such as subcarrier wave QKD, and is also the main aim of Trojan-horse attack for quantum hackers. The key PM component is a lithium niobate electro-optical crystal [31, 32]. Insertion losses and calculated error of measurements for the tested PM are shown in Fig.2.

PM insertion losses increase with the wavelength, which may be attributed to the modulator crystal absorption. Considering errors in insertion loss measurements for forward and backwards directions, these measurements are considered identical. According to its datasheet, losses at 1550 nm are -3 dB which is consistent with our measurements. Losses at longer wavelengths may negatively affect the possibility of Trojan-horse attack. Maximum value of additional losses is -52 dB for 2075 nm in a double-pass scheme.

2. Variable optical attenuators

The second investigated component was a variable optical attenuator (VOA) which is used in Alice's mod-

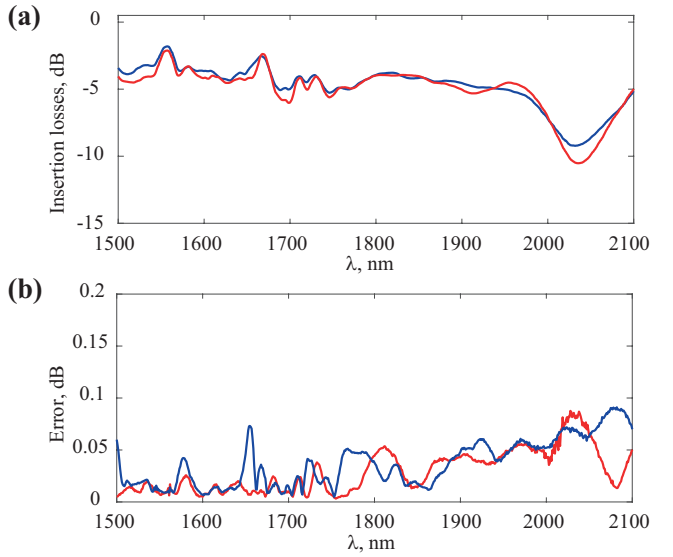


FIG. 4. Measured insertion losses and calculated errors for polarising beam splitter. (a) Insertion losses (blue line is insertion losses for forward direction, red line is insertion losses for backwards direction); (b) calculated errors (blue line is for forward direction, red line is for backwards direction)

ule for setting single photon power level in the quantum channel. Therefore altered VOA functionality may lead to a severe security breach. We measured the properties of two VOAs which differed by switching time and internal structure. Therefore, in this paper we refer to them as electro-optical VOA, and electro-mechanical VOA. The measurements were preformed at two VOA settings: at maximum and minimum attenuation. Attenuation value was changed by altering the control voltage. The results of our measurements are showed in FIG.3.

Insertion losses of the electro-mechanical VOA are relatively stable in a wide spectral range for both minimum and maximum attenuation. The level of attenuation at a set voltage was consistent with its datasheet. Electro-optical VOA insertion losses are also consistent with the datasheet in telecommunication range, but it had an unexpected transmission window with low attenuation beyond this range. For the supplied voltage correspondent to minimal attenuation, electro-optical VOA did not insert any significant losses for 1650 – 1750 nm. For longer wavelengths, attenuation level is lower compared with the datasheet values given for telecom range.

3. Polarising beam splitter

Polarising beam splitter (PBS) is an important optical element for implementing some countermeasures. PBS was also placed in Bob's module of subcarrier wave QKD for dividing polarisation components of the signal for their future modulation. The measurement results are shown in Fig.4.

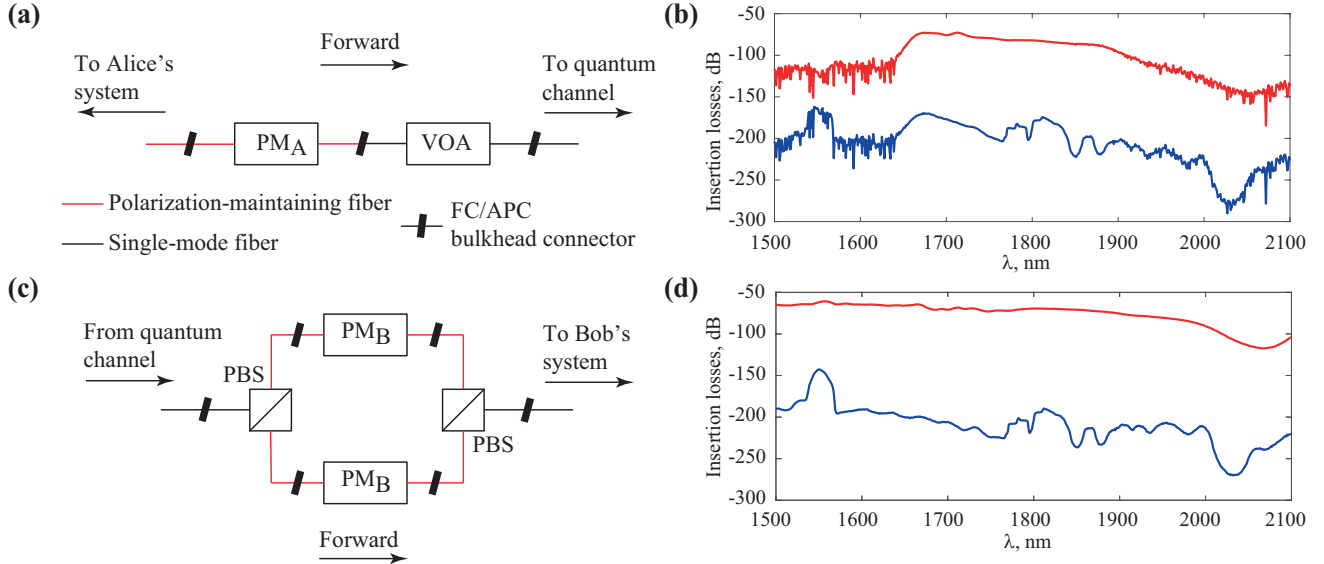


FIG. 5. Insertion losses in studied subcarrier wave QKD optical setups. (a) Studied part of Alice's optical scheme; (b) integral insertion losses in Alice (red line is without any countermeasures, blue line is with countermeasures); (c) Studied part of Bob's optical scheme; (d) integral insertion losses in Bob (red line is without any countermeasures, blue line is with countermeasures)

Insertion losses of PBS were almost the same for each arm and direction: around -5 dB in a wide range from 1500 nm to 2000 nm. We should note that the unpolarized source was used for measurements, thus insertion losses for polarised sources may be even lower.

sured insertion losses of variable optical attenuator, polarising beam splitter and phase modulator, respectively. Index b marks backwards direction. Ref = -50 dB is estimated reflection from the modulator crystal facet, as explained above.

C. Countermeasures

1. Problem

In order to estimate possible Trojan-horse attack efficiency in the wide spectral range we should first identify the part of the optical setup Eve would be probing. Since any optical elements introduce losses, an optimal attack would monitor reflection of the probe as close to the quantum channel as possible, but still after the PM in order to gather the information about signal states. Therefore we presume that Eve would monitor the losses between the quantum channel entrance and the further facet of the PM, which has significant reflectance. These studied parts of Alice's and Bob's optical schemes are shown in FIG.5.

To calculate transmittance in the investigated parts of Alice's and Bob's modules (without any passive countermeasures against quantum hacking) we sum up insertion losses of each measured optical element:

$$T_A = T_{VOAf} + T_{PMf} - \text{Ref} + T_{PMb} + T_{VOAb} \quad (2)$$

$$T_B = T_{PBSf} + T_{PMf} - \text{Ref} + T_{PMb} + T_{PBSb} \quad (3)$$

where T_A and T_B are insertion losses in Alice's and Bob's studied optical paths. T_{VOAf} , T_{PBSf} , T_{PMf} are mea-

By using expressions 2 and 3, we obtained the insertion losses of the studied parts of Alice's and Bob's optical systems, respectively, which are shown in FIG.5. For Alice transmission we used electro-optical VOA data to show possible loopholes beyond telecom range. We found maximum transmission for Alice's system to be -72 dB at 1713 nm. The minimum was -184 dB, at 2072 nm. VOA mostly affects transmission of Alice's system beyond telecom range, but its effect is neglected with by the change in PM transmission. For Bob's system, transmission beyond telecom range decreased with the increase of wavelength. The maximum was at 1805 nm and the minimum was at 2067 nm, with values -69 dB and -117 dB, respectively. Thus, we can conclude that investigated scheme requires additional countermeasures beyond telecom range. To solve these, we used additional elements to increase insertion losses of Alice's and Bob's studied optical paths. In Fig. 5 we also plotted graphs where insertion losses of combination of optical elements are considered as countermeasures, as explained in the next section. In this case we chosen such number of additional elements that insertion losses for investigated schemes were not higher than -140 dB. Calculated errors for these modeling are not higher than 0.5 dB.

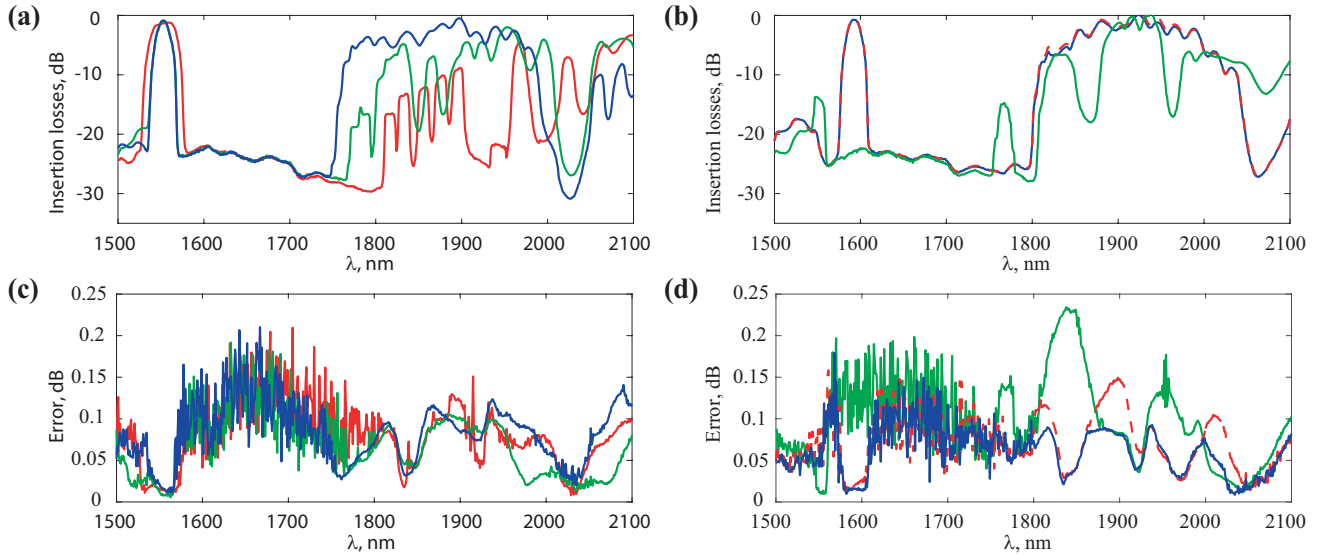


FIG. 6. Measured insertion losses and calculated errors of WDM components. (a) Blue and green lines are same CWDM components from different batches, red line is a CWDM component from another manufacturer; (b) blue line and red dashed line are CWDM components from the same batch, green line is a DWDM component; (c),(d) are calculated errors for the same line colours respectively

2. Possible solutions

There are several ways of preventing Trojan-horse attack, such as using fiber filters based on different filtering principles, circulators, and watchdog detectors. However, unfortunately not all of them are efficient for longer wavelengths, in particular beyond 1800 nm. For that reason we investigated transmission spectra of several optical elements which are conventionally used as quantum hacking countermeasures.

3. Isolators

In many QKD systems isolators ensure decreasing intensity of the outcoming light, such as backscattered light or probe pulses used for Trojan-horse attack. Most of the manufacturers usually indicate the value of backwards attenuation for telecommunication spectrum, but Trojan-horse attack is possible for longer wavelengths. However, an isolator is an example of a fiber optical element with altering properties beyond its normal operating range [11]. That leads to a necessity measuring their transmission in a wider spectral range.

In this study we measured insertion losses of three different isolators: two isolators from the same manufacturer (but different batches) in 1550 nm range and one from another manufacturer in 1310 nm.

For 1550 nm isolators we found that insertion losses in forward direction decreased slowly and not lower than -7 dB (FIG.7). For the 1310 nm isolator they decreased sharply and reached a minimum at 1853 nm, but for telecom range its attenuation was consistent with datasheet.

Backward insertion losses for each isolator decreased with increasing of scanning wavelength, which is consistent with other experimental [27] and theoretical research [33].

4. WDM-components

Another way of introducing additional losses into Eve's probing signals is installing wavelength-division multiplexing (WDM) components that would cut off wavelengths not used by Alice. In our work, we measured transmission of coarse WDM (CWDM) and dense (DWDM) components.

CWDM elements from two different manufacturers were studied. We had three samples from one of the manufacturers, that came from different batches: two from the first (blue straight and red dashed lines in FIG.6b) and one from the second (green line in FIG.6a). The forth CWDM came from another manufacturer (red line in FIG.6a). As can be seen from the figures, each investigated component had wide transmission windows beyond the telecom range. Surprisingly, even though WDM components from the same batch had identical insertion losses, components from different batches had very distinct transmission spectra. These peculiarities could be attributed to production technology of thin film filters [34]. This may potentially affect the security of QKD system and should be always considered. The measured DWDM filter spectrum can also be seen in FIG.6b) (green line) and is similarly characterized by wide transmission windows in 1800 – 2100 nm range.

The collected data clearly indicates that isolators and WDM filters can not easily act as sufficient countermea-

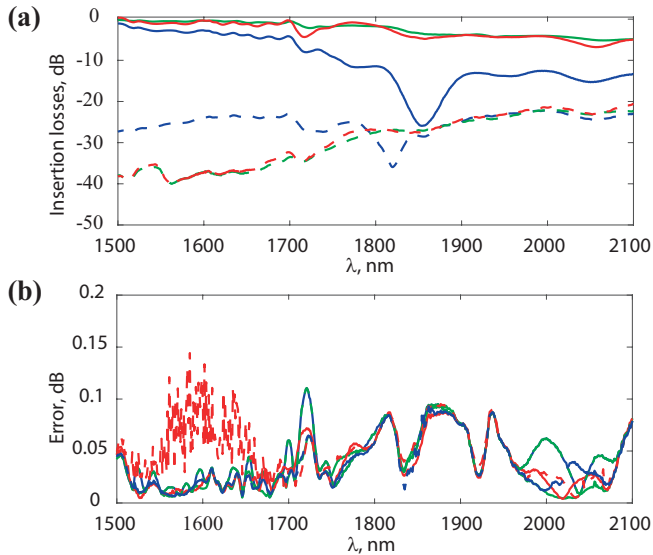


FIG. 7. Measured insertion losses of isolators. (a) In forward direction (straight lines) and backward directions (dashed lines) and (b) their calculated errors, where red and blue lines are for 1550 nm isolators and green lines are for 1310 nm isolator

sures in the investigated spectral region and should be carefully considered and experimentally studied during QKD design.

5. Fiber windings

We therefore suggest creating fiber windings in QKD modules as simple and passive countermeasure to prevent quantum hacking at longer wavelengths. It is known that macrobending losses in single-mode fiber increase with wavelength. Thus, a section of fiber of certain length, bent at a certain radius can act as a spectral filter. To demonstrate this, we installed 1 m of single-mode optical fiber with different windings in our QKD kits to measure their transmission. The results can be seen in Figure 8.

The windings have low effect at transmission around 1550 nm, QKD system operating wavelength. At the same time, for the longer wavelengths, in particular beyond 1830 nm, it introduces up to 30 dB loss in one direction for the bending radius of 24 mm. As a result, this simple technique is a good optical probing countermeasure beyond standard telecommunication wavelength range.

III. THEORETICAL CALCULATIONS AND ANALYSIS

As a result of Trojan-horse attack an eavesdropper can receive some additional to the attacks on quantum channel information. To analyse an eavesdropper's advantage given by the considered attack we need to estimate the

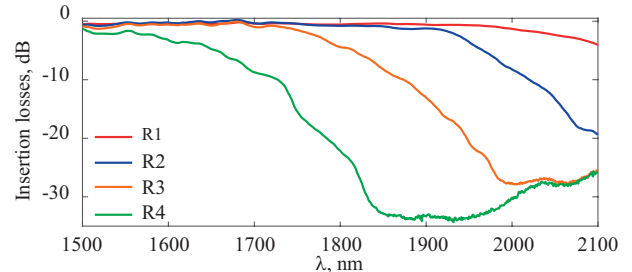


FIG. 8. Single-mode fiber transmission with different winding radii (R1 is 60 mm, R2 is 42 mm, R3 is 36 mm, R4 is 24 mm)

output power from both Alice and Bob. Depending on it we can calculate the efficiency of the attack. Maximum amount of information that can be obtained from the output can be easily evaluated after reconciliation step using Holevo bound as follows:

$$\chi = S \left(\sum_k p_k \rho_k \right) - \sum_k p_k S(\rho_k), \quad (4)$$

where $S(\rho) = -Tr(\rho \log \rho)$ is von Neumann entropy, ρ_k is the density matrix of one state from the set and p_k denotes *a priori* probability of the k -th state. However, since we consider the SCW QKD system and the set of pure states the Eq. 4 can be rewritten as it was shown in paper [35] as follows:

$$\chi(\mu) = h \left(\frac{1 - \langle \psi(0) | \psi(\pi) \rangle}{2} \right) \approx h \left(\frac{1 - e^{-2\mu}}{2} \right), \quad (5)$$

where $h(x) = -x \log_2(x) - (1-x) \log_2(1-x)$ is binary entropy function, $|\psi(\phi)\rangle$ is a quantum state modulated with harmonic electrical signal that has phase ϕ , and μ is the mean photon number of all sidebands in the spectrum.

Upper bound on allowed power of light in an optical fiber is approximately 10 Wt, at this point laser can initiate fiber fuse [10, 23, 36]. We will use the latter value as the upper bound of the input power by an eavesdropper. This amount of power should be scaled by total insertion losses T and then converted to the mean number of photons in order to obtain the mean number of photons of output light. For example, 12.8 pW power at 1550 nm wavelength corresponds to 0.1 mean photon number at 100 MHz repetition (phase change) rate. Also, one should keep in mind that only sidebands contain information about chosen by legitimate party phase, hence ratio $M < 1$ of power of the sidebands to all optical power should be taken into account. Thus, mean photon number of an output probe beam can be estimated by:

$$\mu_p = \frac{M \cdot 0.1 \cdot 10 \cdot 10^{\frac{T}{10}}}{12.8 \cdot 10^{-12}} \approx M \cdot 10^{\frac{T}{10} + 10.93}. \quad (6)$$

For further numerical estimations we assume $M = 0.1$. Then it is straightforward that $\chi(\mu_p)$ is an upper bound

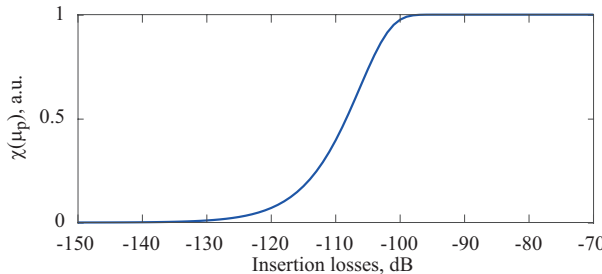


FIG. 9. Holevo bound (5) evaluated for mean photon number of an output probe beam, μ_p (6), dependent on insertion losses

estimation on eavesdropper's information that should be taken into account at the step of privacy amplification. In Fig. 9 dependence of $\chi(\mu_p)$ on total insertion losses T is shown. For $T > -100$ dB eavesdropper may obtain almost all key information, while obtained information is rather small for $T < -130$ dB. One may compare these values to the ones shown in Fig. 5(b) and (d), where insertion losses is not higher than negative 140 – 150 dB. The latter values of insertion losses correspond to $\chi < 10^{-3}$, that should be taken into consideration at the privacy amplification step.

IV. CONCLUSION

In this paper we have experimentally investigated the spectral properties of conventional QKD components: phase modulators, variable attenuators, isolators, CWDM and DWDM filters, in a spectral range of 1550 – 2100 nm. We have shown that transmission of

various fiber optical elements beyond telecommunication range (especially 1800 nm and beyond) should be taken into account during QKD system design because of the possibility for realization of Trojan-horse attack, as we demonstrate in the brief theoretical analysis. Moreover, even identical optical components from the same manufacturers can have varying optical spectra out of their normal operation range. We also suggested a simple passive countermeasure against Trojan-horse attacks in 1800 – 2100 nm range based on violating the total internal reflection in a bended optical fiber. This technique introduces up to 30 dB additional loss at each passing for the winding radius of 24 mm and insert low losses at 1550 nm.

Combined countermeasures allow us to achieve “secure” region at negative 140 – 150 dB insertion losses, where upper bound estimation on eavesdropper's information (additional to attacks in a quantum channel) is rather low, $\chi < 10^{-3}$. Derived expression $\chi(\mu_p)$, composed by (5) and (6) (or analogous expression suitable for different QKD systems), may be utilized in order to make express-estimations on eavesdropper's information that should be taken into consideration at the privacy amplification step. As an alternative, derived expression $\chi(\mu_p)$ may be utilized for a QKD system's optical design, where one may determine insertion loss threshold keeping χ considerably low.

ACKNOWLEDGMENTS

The study was partially funded by the Ministry of Education and Science of the Russian Federation (Passport No. 2019-0903).

[1] Artur K Ekert. Quantum cryptography and bell's theorem. In *Quantum Measurements in Optics*, pages 413–418. Springer, 1992.

[2] Charles H Bennett, Gilles Brassard, and N David Mermin. Quantum cryptography without bell's theorem. *Physical review letters*, 68(5):557, 1992.

[3] Peter W Shor and John Preskill. Simple proof of security of the bb84 quantum key distribution protocol. *Physical review letters*, 85(2):441, 2000.

[4] Nitin Jain, Hou-Man Chin, Hossein Mani, Cosmo Lupo, Dino Solar Nikolic, Arne Kordts, Stefano Pirandola, Thomas Brochmann Pedersen, Matthias Kolb, Bernhard Ömer, et al. Practical continuous-variable quantum key distribution with composable security. *Nature communications*, 13(1):1–8, 2022.

[5] Yi Zhao, Chi-Hang Fred Fung, Bing Qi, Christine Chen, and Hoi-Kwong Lo. Quantum hacking: Experimental demonstration of time-shift attack against practical quantum-key-distribution systems. *Physical Review A*, 78(4):042333, 2008.

[6] Anqi Huang, Álvaro Navarrete, Shi-Hai Sun, Poompong Chaiwongkhot, Marcos Curty, and Vadim Makarov. Laser-seeding attack in quantum key distribution. *Physical Review Applied*, 12(6):064043, 2019.

[7] Poompong Chaiwongkhot, Jiaqiang Zhong, Anqi Huang, Hao Qin, Sheng-cai Shi, and Vadim Makarov. Faking photon number on a transition-edge sensor. *arXiv preprint arXiv:2102.08746*, 2021.

[8] SN Molotkov, KA Balygin, AN Klimov, and SP Kulik. Active sensing and side channels of information leakage in quantum cryptography. *Laser Physics*, 29(12):124001, 2019.

[9] Paulo Vinicius Pereira Pinheiro, Poompong Chaiwongkhot, Shihan Sajeed, Rolf T Horn, Jean-Philippe Bourgoin, Thomas Jennewein, Norbert Lütkenhaus, and Vadim Makarov. Eavesdropping and countermeasures for backflash side channel in quantum cryptography. *Optics express*, 26(16):21020–21032, 2018.

[10] Anqi Huang, Ruoping Li, Vladimir Egorov, Serguei Tchouragoulov, Krtin Kumar, and Vadim Makarov. Laser-damage attack against optical attenuators in quantum key distribution. *Physical Review Applied*, 13(3):034017, 2020.

[11] Anastasiya Ponosova, Daria Ruzhitskaya, Poompong

Chaiwongkhot, Vladimir Egorov, Vadim Makarov, and Anqi Huang. Protecting fiber-optic quantum key distribution sources against light-injection attacks. *PRX Quantum*, 3:040307, Oct 2022.

[12] Artem Vakhitov, Vadim Makarov, and Dag R Hjelme. Large pulse attack as a method of conventional optical eavesdropping in quantum cryptography. *Journal of modern optics*, 48(13):2023–2038, 2001.

[13] Nicolas Gisin, Sylvain Fasel, Barbara Kraus, Hugo Zbinden, and Grégoire Ribordy. Trojan-horse attacks on quantum-key-distribution systems. *Physical Review A*, 73(2):022320, 2006.

[14] Nitin Jain, Elena Anisimova, Imran Khan, Vadim Makarov, Christoph Marquardt, and Gerd Leuchs. Trojan-horse attacks threaten the security of practical quantum cryptography. *New Journal of Physics*, 16(12):123030, 2014.

[15] Shihan Saeed, Igor Radchenko, Sarah Kaiser, Jean-Philippe Bourgoin, Anna Pappa, Laurent Monat, Matthieu Legré, and Vadim Makarov. Attacks exploiting deviation of mean photon number in quantum key distribution and coin tossing. *Physical Review A*, 91(3):032326, 2015.

[16] Yaxi Pan, Ling Zhang, and Duan Huang. Practical security bounds against trojan horse attacks in continuous-variable quantum key distribution. *Applied Sciences*, 10(21):7788, 2020.

[17] Vadim Makarov. Controlling passively quenched single photon detectors by bright light. *New Journal of Physics*, 11(6):065003, 2009.

[18] Lars Lydersen, Mohsen K Akhlaghi, A Hamed Majedi, Johannes Skaar, and Vadim Makarov. Controlling a superconducting nanowire single-photon detector using tailored bright illumination. *New Journal of Physics*, 13(11):113042, 2011.

[19] Vladimir Chistiakov, Anqi Huang, Vladimir Egorov, and Vadim Makarov. Controlling single-photon detector id210 with bright light. *Optics express*, 27(22):32253–32262, 2019.

[20] Anton Kozubov, Andrei Gaidash, and George Miroshnichenko. Quantum control attack: towards joint estimation of protocol and hardware loopholes. *Physical Review A*, 104(2):022603, 2021.

[21] Andrei Gaidash, George Miroshnichenko, and Anton Kozubov. Subcarrier wave quantum key distribution with leaky and flawed devices. *JOSA B*, 39(2):577–585, 2022.

[22] M.K. Barnoski, M.D. Rourke, S.M. Jensen, and R.T. Melville. Optical time domain reflectometer. *Applied optics*, 16(9):2375–2379, 1977.

[23] Raman Kashyap. The fiber fuse-from a curious effect to a critical issue: A 25 th year retrospective. *Optics Express*, 21(5):6422–6441, 2013.

[24] Nitin Jain, Birgit Stiller, Imran Khan, Vadim Makarov, Christoph Marquardt, and Gerd Leuchs. Risk analysis of trojan-horse attacks on practical quantum key distribution systems. *IEEE Journal of Selected Topics in Quantum Electronics*, 21(3):168–177, 2014.

[25] Ivan S Sushchev, Diana M Guzairova, Andrey N Klimov, Dmitriy A Dvoretskiy, Sergey A Bogdanov, Klim D Bondar, and Anton P Naumenko. Practical security analysis against the trojan-horse attacks on fiber-based phase-coding qkd system in the wide spectral range. In *Emerging Imaging and Sensing Technologies for Security and Defence VI*, volume 11868, pages 57–63. SPIE, 2021.

[26] Shihan Saeed, Carter Minshull, Nitin Jain, and Vadim Makarov. Invisible trojan-horse attack. *Scientific reports*, 7(1):1–7, 2017.

[27] AV Borisova, BD Garmaev, IB Bobrov, SS Negodyaev, and IV Sinil'shchikov. Risk analysis of countermeasures against the trojan-horse attacks on quantum key distribution systems in 1260–1650 nm spectral range. *Optics and Spectroscopy*, 128(11):1892–1900, 2020.

[28] BA Nasedkin, IM Filipov, AO Ismagilov, VV Chistiakov, FD Kiselev, AN Tsyplkin, and VI Egorov. Analyzing transmission spectra of fiber-optic elements in the near ir range to improve the security of quantum key distribution systems. *Bulletin of the Russian Academy of Sciences: Physics*, 86(10):1164–1167, 2022.

[29] Anton V Tausenev, Petr Georgievich Kryukov, Mikhail Mikhailovich Bubnov, Mikhail Evgen'evich Likhachev, E Yu Romanova, Mikhail Viktorovich Yashkov, Vladimir Fedorovich Khopin, and M Yu Salganskii. Efficient source of femtosecond pulses and its use for broadband supercontinuum generation. *Quantum Electronics*, 35(7):581, 2005.

[30] Shihan Saeed, Poompong Chaiwongkhot, Anqi Huang, Hao Qin, Vladimir Egorov, Anton Kozubov, Andrei Gaidash, Vladimir Chistiakov, Artur Vasiliev, Artur Gleim, et al. An approach for security evaluation and certification of a complete quantum communication system. *Scientific Reports*, 11(1):1–16, 2021.

[31] Ashutosh Rao and Sasan Fathpour. Heterogeneous thin-film lithium niobate integrated photonics for electrooptics and nonlinear optics. *IEEE Journal of Selected Topics in Quantum Electronics*, 24(6):1–12, 2018.

[32] Ed L Wooten, Karl M Kissa, Alfredo Yi-Yan, Edmond J Murphy, Donald A Lafaw, Peter F Hallemeier, David Maack, Daniel V Attanasio, Daniel J Fritz, Gregory J McBrien, et al. A review of lithium niobate modulators for fiber-optic communications systems. *IEEE Journal of selected topics in Quantum Electronics*, 6(1):69–82, 2000.

[33] Michał Berent, Andon A Rangelov, and Nikolay V Vitanov. Broadband faraday isolator. *JOSA A*, 30(1):149–153, 2013.

[34] Pei-fu Gu and Zhen-rong Zheng. Design of non-polarizing thin film edge filters. *Journal of Zhejiang University-SCIENCE A*, 7(6):1037–1040, 2006.

[35] GP Miroshnichenko, AV Kozubov, AA Gaidash, AV Gleim, and DB Horoshko. Security of subcarrier wave quantum key distribution against the collective beam-splitting attack. *Optics express*, 26(9):11292–11308, 2018.

[36] Donald D Davis Jr, Stephen C Mettler, and David J Di-Giovanni. Comparative evaluation of fiber fuse models. In *Laser-Induced Damage in Optical Materials: 1996*, volume 2966, pages 592–606. SPIE, 1997.